

Cationic photopolymerization of cyclic esters at elevated temperatures and their application in hot lithography

Yazgan Mete,^a Konstanze Seidler,^b Christian Gorsche,^b Thomas Koch,^c Patrick Knaack^a and Robert Liska^{a*}



Abstract

The 3D printing of polyesters is most commonly performed using polylactide filaments for material extrusion (formerly known as fused-deposition modelling) or by introducing methacrylate end-groups to polyesters, which can be polymerized by a radical mechanism. However, cyclic esters can also be polymerized via cationic ring-opening photopolymerization, which opens up the possibility of using high-resolution stereolithography as the method of choice to form polyester networks *in situ* during the printing process. Hereby, we present the first approach to 3D print polyesters starting directly from ϵ -caprolactone via stereolithography at elevated temperatures, by introducing low amounts of crosslinks into the material to provide stability to the structure but maintain its degradable character and especially semicrystallinity. Photorheology tests showed that high temperatures and the introduction of crosslinkers led to increased reactivity and fast gelation. By performing tensile tests, dynamic mechanical thermal analysis and simultaneous thermal analysis the material properties were evaluated depending on the amount and type of crosslinker. It was shown that decreasing the amount of crosslinker significantly increased the crystallinity and influenced the mechanical properties as well as shape memory properties. Finally, successful 3D printing of a polyester was performed using 10 mol% of a crosslinker with oxetane moieties and 90 mol% ϵ -caprolactone at 120 °C.

© 2022 The Authors. *Polymer International* published by John Wiley & Sons Ltd on behalf of Society of Industrial Chemistry.

Supporting information may be found in the online version of this article.

Keywords: cyclic esters; crosslinked polyesters; photorheology; shape memory; stereolithography; 3D printing

INTRODUCTION

Photopolymerization is best known for its application in protective and decorative coatings and enables the synthesis of polymers with exceptional mechanical, chemical and thermal stability. In particular, cationic photopolymerization allows on demand initiation and represents a low-energy technique compared to thermal curing. However, recently, the scope of cationic photopolymerization has been extended to more advanced technologies such as additive manufacturing. While radical photopolymerization has long been established in stereolithography-based 3D printing, only few studies use purely cationic techniques. One example is presented by Dall'Argine *et al.*,¹ who printed epoxy resins at elevated temperatures using a triarylsulfonium photoacid generator (PAG). Similarly, the first example of 3D printed 2-oxazolines at temperatures above 100 °C is shown by Klikovits *et al.*²

The key to both these publications is the use of a 3D printing technique, where the process is conducted at elevated temperatures. This additive manufacturing technique, called hot lithography, is equipped with a heated vat where highly viscous monomers can be processed. However, even though the initial aim of this approach was to increase the processability of viscous

compounds at temperatures up to 120 °C, it is also a possibility to increase the polymerization rate of monomers with moderate reactivity at ambient temperatures. With this technique even novolaks have already been used in additive manufacturing.³ One group of monomers, which is abundantly used and crucial in many applications where biocompatibility or biodegradability is required, are cyclic esters. While it is common to polymerize them via anionic ring-opening polymerization, the use of cationic ring-opening polymerization (CROP) is less investigated. Some researchers have already reported the successful CROP of lactones using triarylsulfonium salts^{4,5} or a reversible merocyanine-based visible light regulated PAG.^{6,7} Our recent studies as well as a recently published study from Yagci and colleagues⁸ showed

* Correspondence to: R Liska, Institute of Applied Synthetic Chemistry, TU Wien, Getreidemarkt 9/163 MC, 1060 Vienna, Austria. E-mail: robert.liska@tuwien.ac.at

a Institute of Applied Synthetic Chemistry, TU Wien, Vienna, Austria

b Cubicure GmbH, Vienna, Austria

c Institute of Materials Science and Technology, TU Wien, Vienna, Austria

that iodonium salts are also appropriate photoinitiators for different cyclic esters.⁹

When it comes to additive manufacturing, several aspects such as reaction speed, the viscosity of the monomers, volatility and functionality have to be considered.¹⁰ There are two common approaches to 3D print polyesters. In a material extrusion process, the polyester is prepared prior to the printing via conventional polymerization techniques and provided as filaments, which can be melted and transformed to the desired shape. In lithography-based techniques such as digital light processing (DLP) or stereolithography, again the polyester is synthesized before the printing process but modified with acrylate or methacrylate end-groups, to introduce moieties that can be polymerized with radical photoinitiators. The deployment of polycaprolactone capped with methacrylate end-groups in a DLP process is shown by Invernizzi *et al.*, who also show the self-healing and shape memory properties of the material.¹¹ Others follow a similar approach using methacrylic end-groups to perform stereolithography.^{12,13} Thompson *et al.* even use polycaprolactone with acrylate end-groups in a two-photon polymerization process, building biocompatible retinal-cell-delivery scaffolds.¹⁴ Lammel-Lindemann *et al.* prepare isosorbide-based unsaturated polyesters and use the double bonds as crosslinking sites during the DLP process.¹⁵ Polymerizable double bonds have also been introduced to the terminal moieties of the polymer backbone, by using acryloyl chloride,¹⁶ itaconic anhydride¹⁷ or fumaric acid monoethylester.¹⁸

Overall, to the best of our knowledge, no attempts to directly use ϵ -caprolactone (ϵ CL) or other cyclic esters in a photopolymerization process to 3D print parts have been made. Therefore, this work aims to investigate the possibility of using the cationic photopolymerization of cyclic esters and circumventing the prior preparation of a modified polyester. Based on a previous study⁹ ϵ CL was selected as an appropriate lactone and its reactivity was tested in combination with bifunctional monomers in photorheology experiments. After establishing a reactive system, the crosslinked polyester specimens were analysed via tensile tests and dynamic mechanical thermal analysis (DMTA). Finally, we present the first proof of concept that cyclic esters can directly be printed using CROP at elevated temperatures.

RESULTS AND DISCUSSION

Selection of monomers

In our previous evaluation of four- to eight-membered cyclic esters, ϵ CL was selected as the most appropriate monomer for reactions at elevated temperatures using an iodonium salt as the PAG. The compound was singled out due to its better storage stability, good reactivity, higher boiling point and low price.⁹ Since the printing requires some time and the thermal stability of the formulations during the process is crucial, a sulfonium salt (sulfonium-based photoinitiator Irgacure 290 from BASF (S-B)) (Fig. 1) was used as the initiator. Based on the same considerations, a similar choice was made by Dall'Argine *et al.*¹ and Klinkovits *et al.*² for the hot lithography of epoxides and 2-oxazolines.

In order to introduce crosslinks and form a stable structure very early in the polymerization, difunctional compounds were added. The critical aspects of selecting a crosslinker and the amount thereof were the successful copolymerization with the monofunctional compound and the material properties of the product. While more crosslinker leads to a faster gelation and therefore a stable structure is formed faster during printing, it also means that the crystallinity of the material is decreased, which significantly

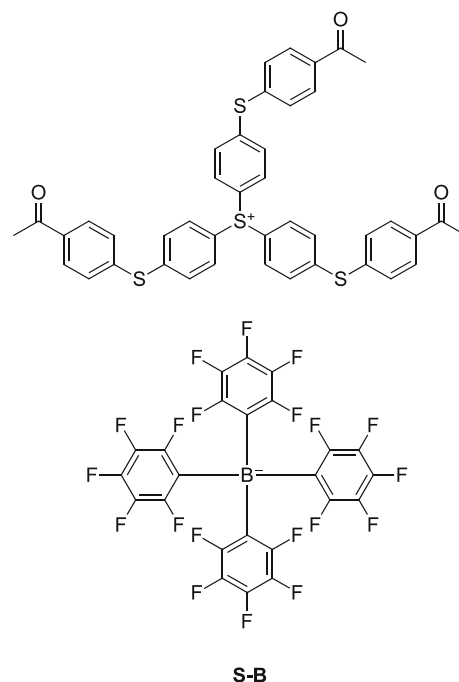


Figure 1. The sulfonium-based photoinitiator Irgacure 290 from BASF (S-B).

changes the material properties. Therefore, studies were conducted to single out a crosslinker that leads to fast gelation and to determine the right amount which needs to be added, to conduct 3D printing experiments. The tested crosslinkers included synthesized as well as commercially available ones and are presented in the following sections.

Synthesis of a difunctional cyclic ester as crosslinker

The preparation of the difunctional crosslinker [4,4'-bioxepane]-7,7'-dione, which will be referred to as DCL, was performed according to the one-step procedure described by Palmgren *et al.* (Fig. 2).¹⁹ The commercially available ketone 4,4'-bicyclohexanone was dissolved in dichloromethane, cooled down in an ice-bath and oxidized by adding *m*-chloroperoxybenzoic acid (mCPBA) in excess while stirring.

The crude reaction mixture was then extracted and the crude product was purified via recrystallization from ethyl acetate, yielding a white solid (80%). Since the monomer is not liquid and exhibits a very high melting point, it could only be used in combination with other monomers which act as a solvent for the crosslinker. Additionally, only low amounts of the crosslinker could be used due to the poor solubility despite carefully heating up the mixture.

Photoreology analysis of network formation with crosslinkers

When parts are 3D printed via stereolithography, it is crucial that gelation occurs fast and gives the printed material stability, so that additional layers can be added. The most straightforward way would be using a multifunctional monomer bearing the same moieties as the monofunctional compound, such as DCL. However, if copolymerization occurs with other functional groups, the possibilities expand and additional commercially available monomers can be considered. The copolymerization of epoxides and ϵ CL has already been reported by Sangermano *et al.*, where

bisphenyl A glycidyl ether (BADGE) was used as crosslinker.⁴ Oxetanes, which are also cyclic ethers, polymerize by the same mechanism and our preliminary tests confirmed that copolymerization with ϵ CL is occurring. Figure 3 shows the proposed mechanism for the acid catalysed copolymerization of ϵ CL with an oxetane.

The initial photorheology analysis aimed to single out the most appropriate crosslinker for the polymerization with ϵ CL. Considering that fast gelation is desired, the most important aspect was the polymerization speed.

In addition to the synthesized crosslinker DCL, four commercially available compounds were selected for the analysis (Fig. 4). Photorheology has been established as an excellent technique to observe the development of the storage (G') and loss (G'')

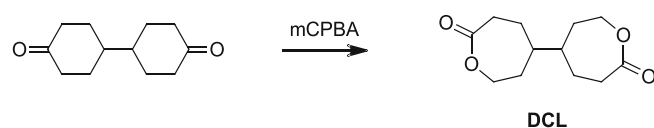


Figure 2. Baeyer–Villiger oxidation of 4,4'-bicyclohexanone to a difunctional cyclic ester (DCL).

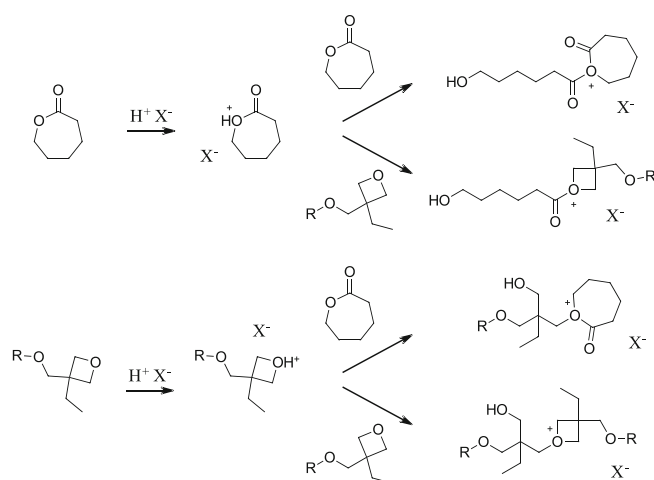


Figure 3. Copolymerization of caprolactone with an oxetane via acid catalysis.

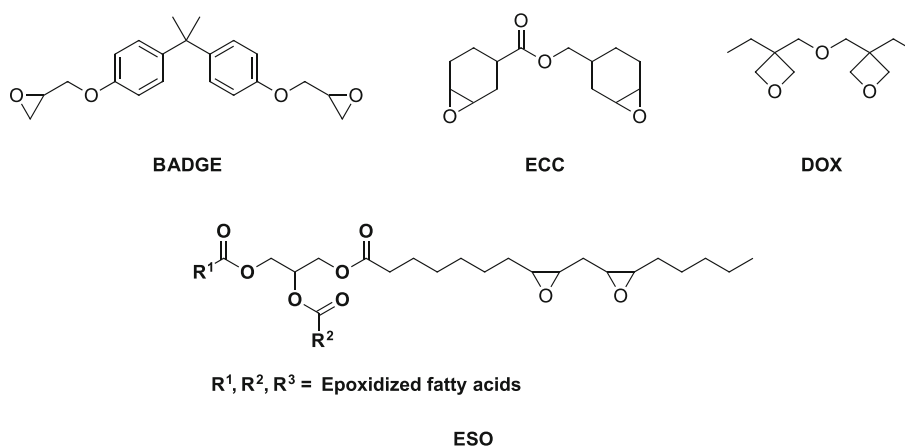


Figure 4. Bisphenol A diglycidyl ether (BADGE), 3,4-epoxycyclohexylmethyl-3',4'-epoxycyclohexancarboxylate (ECC), 3,3'-[oxybis(methylene)]bis[(3-ethyl)oxetane] (DOX) and epoxidized soybean oil (ESO).

moduli during photoinduced curing.^{20,21} Using their intersection the gelation time of the polymerization (t_{gel}) can be determined. Since gelation plays a major role in the printing process, t_{gel} gives crucial information about the minimum irradiation time.²² The photorheology measurements were conducted at 100 °C with 1 mol% S-B relative to the number of functional groups.

The obtained data clearly show that, among all tested crosslinkers, 3,3'-[oxybis(methylene)]bis[(3-ethyl)oxetane] (DOX) reacts the fastest and also reaches the highest final storage modulus (Fig. 5) (Table 1). Also, significant differences between the three epoxy monomers can be observed, where BADGE shows the highest delay and slowest polymerization rate. While it is surprising that epoxidized soybean oil (ESO) seems to react faster than BADGE, the slow reaction of BADGE can be explained by the formation of a proton clamp, which slows down the initiation. The difunctional cyclic ester DCL leads to a significantly slower polymerization, but the solubility issues with the solid crosslinker can be immediately seen when looking at the high storage modulus at the beginning of the polymerization. While measurements with 5 mol% were easier to perform, 10 mol% of DCL seems to show precipitation even at 100 °C (Fig. S1). Nevertheless, the increased G' upon polymerization can be observed around 170 s. Determining the gel point proved to be challenging with these formulations since the intersection of the storage (G') and loss (G'') moduli curves either appeared with a delay or in some measurements could not be determined at all. However, to have a comparable value for all measurements, the time until G' reached 100 Pa was measured, since this value appeared to be reproducible throughout all tests, except for DCL which showed an increased G' from the beginning due to precipitation. Based on these results, DOX and DCL were selected as suitable crosslinkers for further studies, DOX for the good results obtained and DCL—even though more difficult to deploy—because it represents the only crosslinker with the same functional groups as the monofunctional monomer.

Despite using simultaneous real time Fourier transform IR measurements for conversion analysis during the curing process, it was not possible to identify the relevant absorption peaks due to superposition with other peaks. The same problem was observed during the copolymerization of epoxides and ϵ CL by Sangermano *et al.*⁴

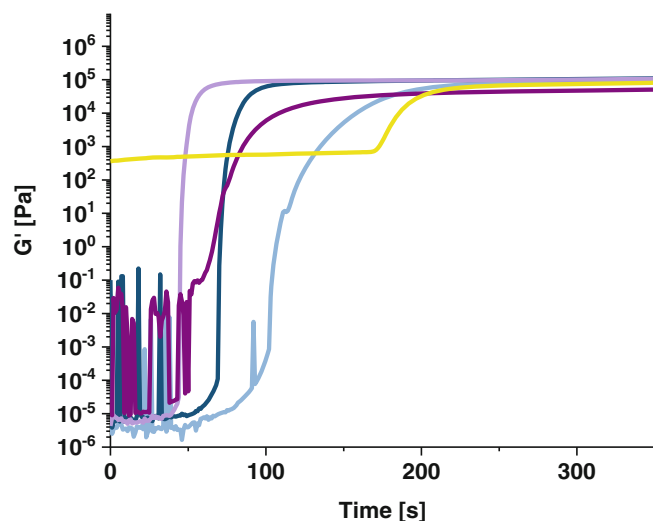


Figure 5. Storage modulus (G') for formulations consisting of 90% ϵ CL and 10% BADGE (light blue), ECC (dark blue), ESO (purple), DOX (violet) and DCL (yellow) cured at 100 °C with 1 mol% of S-B with respect to the functional groups.

Table 1. Photoreology results for formulations consisting of 90% ϵ CL and 10% of the respective crosslinker cured with 1 mol% S-B

Crosslinker 10 mol%	$t_{G>100}$ (s)	G'_{final} (MPa)
BADGE	113 ± 7	0.13 ± 0.004
ECC	72 ± 3	0.14 ± 0.002
ESO	72 ± 2	0.064 ± 0.0005
DOX	43 ± 0	0.14 ± 0.003
DCL	–	0.12 ± 0.0009

The value $t_{G>100}$ represents the time until the storage modulus reaches 100 Pa. G'_{final} is the storage modulus of the final plateau.

Dynamic mechanical thermal analysis (DMTA)

The specimens for mechanical tests were not only cured via UV light but also thermally in an additional post-curing step, to ensure full conversion. Another reason for the post-curing was that 3D printed parts are commonly post-cured via thermal and/or UV treatment to further increase the final conversion of the printed part. Visually, it can be seen that samples containing 5% of crosslinker changed their appearance from translucent to opaque after a certain amount of time, due to increased crystallinity, while the samples with 10% stayed the same. Therefore, for mechanical tests, two groups of specimens were prepared, where one group was measured 1 day after polymerization and the second group was measured after being stored 4 weeks at room temperature. The results from the DMTA analysis using DOX as crosslinker (Fig. 6(a)) show that specimens containing 5% crosslinker have a more distinct melting behaviour around 55 °C and a higher crystallinity once they are stored for a longer time. Also, there is a significant shift of the T_g (Fig. 6(b)) to higher temperatures. When the samples containing 5% crosslinker are measured shortly after polymerization (blue dotted line), they exhibit a behaviour that is more similar to the amorphous samples containing 10% crosslinker. Contrary to that, there is no change when the samples with 10% crosslinker are stored for 4 weeks. These samples have generally a better defined T_g , but turn very soft at higher

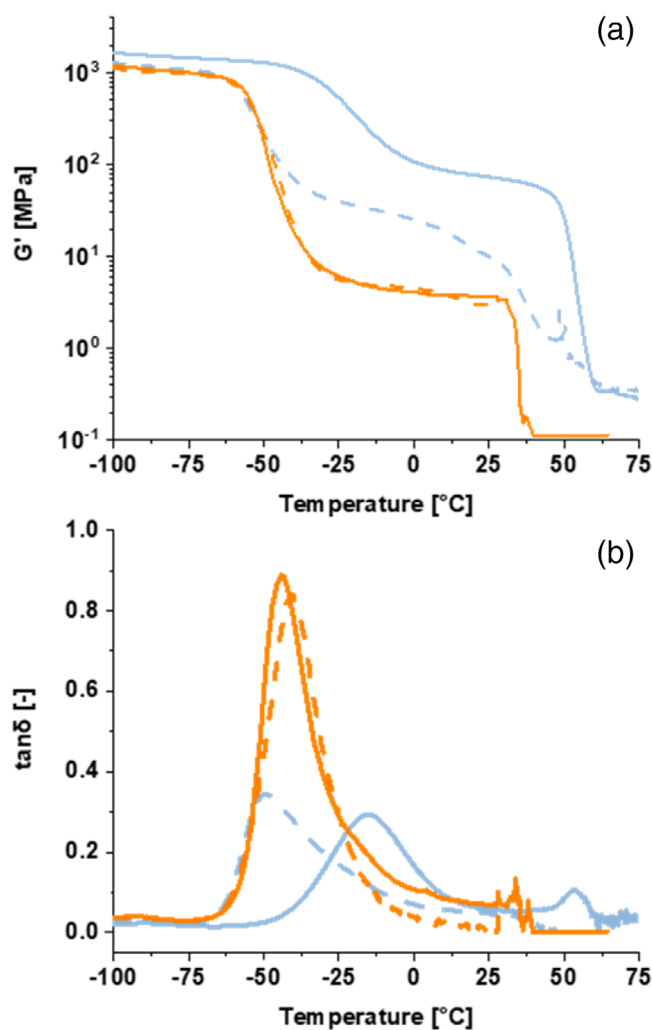


Figure 6. (a) Storage moduli (G') and (b) loss factor ($\tan \delta$) of DMTA specimens containing ϵ CL and 5% (light blue) or 10% (orange) DOX after 1 day (broken lines) and 4 weeks (full lines) of storage.

temperatures, so that the measurements had to be interrupted earlier than for samples containing 5 mol%. The crystalline samples on the other hand have a more distinct melting point, which corresponds to the melting point of the polycaprolactone homopolymer.

The data obtained from the DMTA are summarized in Table 2. The full-width at half-maximum values describe the width of the $\tan \delta$ curve and represent the homogeneity of the network. Lower values for samples with more crosslinker indicate a more homogeneous network. At the same time, the storage modulus at the rubber plateau is significantly reduced. The highest G' values at 25 °C and the rubber plateau (G'_r) are achieved by the sample with the highest crystallinity, which is the 5 mol% DOX sample stored for 4 weeks.

The same tests were repeated using DCL as crosslinker. Due to solubility issues, the preparation of the specimens proved to be more challenging than using DOX. While higher temperatures improved the solubility, the cured samples showed a less even surface when the formulations were heated during irradiation. Also, in order to avoid evaporation, the irradiation had to be performed more carefully and stepwise. In addition, softer materials were more difficult to remove from the moulds and all samples

Table 2. Summarized values for G'_{25} (storage modulus at 25 °C), T_g (glass transition temperature), fwhm (full-width at half-maximum of the $\tan \delta$ curve) and G'_r (storage modulus at the rubber plateau) from the DMTA measurement of samples containing 5 or 10 mol% DOX

DOX	Storage	G'_{25} (MPa)	$\tan \delta_{\max}/T_g$ (°C)	fwhm (°C)	G'_r (MPa)
5 mol%	1 day	10.0	-49.3	32.7	24.7
	4 weeks	73.5	-15.5	33.6	65.5
10 mol%	1 day	3.0	-40.8	20.8	4.0
	4 weeks	3.7	-44.1	19.5	3.9

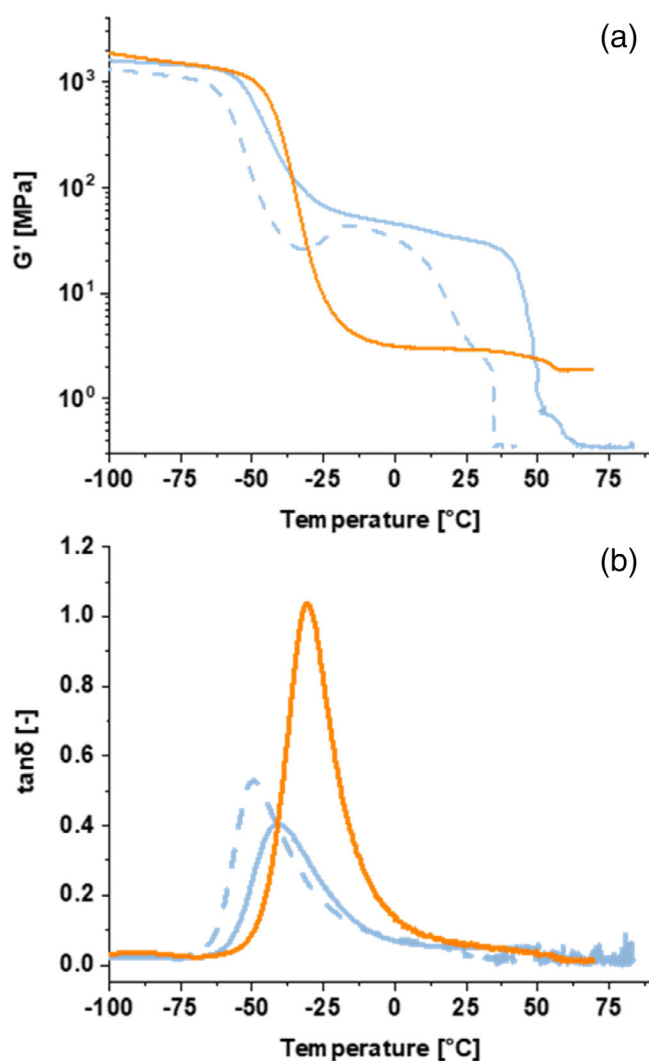


Figure 7. (a) Storage moduli (G') and (b) loss factor ($\tan \delta$) of DMTA specimens containing ϵ CL and 5% (light blue) or 10% (orange) DCL after 1 day (broken lines) and 4 weeks (full lines) of storage.

containing 10 mol% of difunctional cyclic ester DCL tore apart when they were separated from the mould 1 day after polymerization. Hence, the 10% sample was only measured after 4 weeks. Again, the data show that the crystallinity of the material is still developing over time (Fig. 7, Table 3). Samples with 5 mol% crosslinker show a significant shift of T_g to higher temperatures after 4 weeks and an increase of storage modulus. After 50 °C, the measurements were disrupted since the materials turned very soft. However, shortly before, it can be seen that samples with

5 mol% DCL exhibit a clear melting point contrary to samples with high crosslinker content and therefore lower crystallinity.

Conversion analysis

As mentioned in the section **Photorheology analysis of network formation with crosslinkers**, the conversion of the crosslinked samples was not analysed via near or mid IR analysis since the relevant signals could not be observed or integrated without an overlap of other peaks. Attempts to use deconvolution software were also unsuccessful. Therefore, small parts of the DMTA samples were cut off immediately after post-curing and put in methyl ethyl ketone (MEK) in order to leach out residual monomers or homopolymers. After 24 h the samples were removed, dried and the soluble parts were analysed via NMR and gel permeation chromatography (GPC) after removing the solvent. Overall, no residual monomers could be found, but homopolymers of ϵ CL with molecular weights up to 1500 g mol⁻¹ were isolated, which were not integrated into the network and could therefore be leached out of the samples. Gravimetric analysis showed that approximately 21 ± 1.6 wt% of the samples with 10 mol% crosslinker and 24 ± 1.2 wt% of the samples with 5 mol% crosslinker consisted of soluble homopolymers. In samples with DCL the homopolymers reached molecular weights up to 2700 g mol⁻¹.

Simultaneous thermal analysis (STA)

The DMTA measurements already showed significant differences between the specimens, which are derived from the degree of crystallinity. To have a more accurate thermal analysis, small parts of the DMTA specimens that were stored for 4 weeks were heated in the DSC device up to 250 °C to determine the melting enthalpy of the crystalline phases. The curves obtained (Fig. 8) confirm that there is a significant difference in the melting enthalpy. For estimation of the crystallinity, the heat of fusion for polycaprolactone (-157 J g⁻¹)²³ was used, which results in a crystallinity percentage of 51% for 5 mol% DOX and 18% for 10 mol% DOX.

Again, with DCL, using 10 mol% led to a very similar result. Using 5 mol% of the cyclic ester crosslinker DCL significantly increased the crystallinity. The summarized results in Table 4 show that with 5 mol% DCL crystallinity shares up to 79% were achieved.

Tensile tests

Tensile tests were performed to analyse the maximum stress and the strain at break of the specimens, which were prepared similarly to the DMTA specimens. The observations made with the tensile tests are similar to those made with the DMTA. Again, there is a significant difference for samples containing 5% crosslinker depending on the time of storage after polymerization. Once the crystallinity increases, the samples are more brittle and less strain can be applied before the sample breaks. Furthermore, the specimens containing 10% crosslinker show a more elastic behaviour and a higher strain at break (Fig. 9, Table S1). Generally,

Table 3. Summarized values for G'_{25} (storage modulus at 25 °C), T_g (glass transition temperature), fwhm (full-width at half-maximum of the $\tan \delta$ curve) and G'_r (storage modulus at the rubber plateau) from the DMTA measurements of samples containing 5 or 10 mol% DCL

DCL	Storage	G'_{25} (MPa)	$\tan \delta_{\max}/T_g$ (°C)	fwhm (°C)	G'_r (MPa)
5 mol%	1 day	9.95	-49.3	32.7	24.7
	4 weeks	73.5	-15.5	33.6	65.5
10 mol%	4 weeks	2.9	-30.6	20.2	2.9

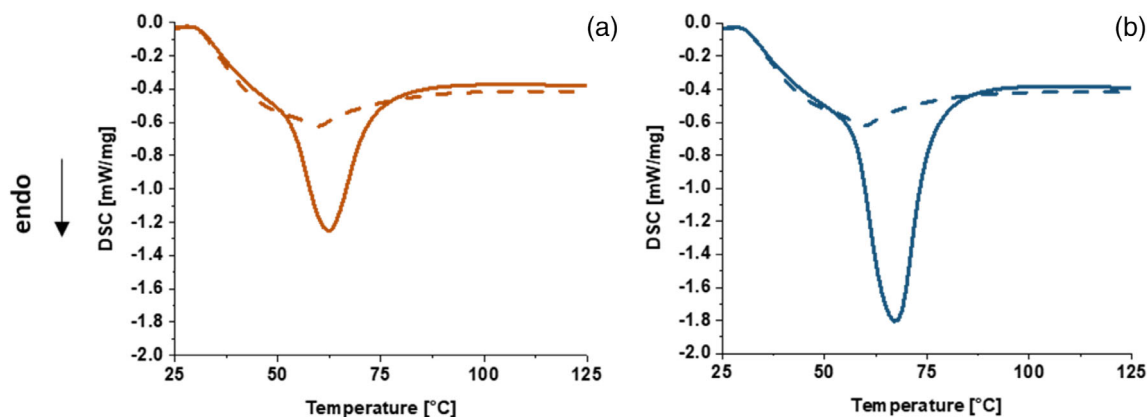


Figure 8. STA of DMTA specimens containing (a) ϵ CL and 5 (full line—) or 10 (broken line---) mol% DOX as crosslinker and (b) ϵ CL and 5 (full line—) or 10 (broken line---) mol% DCL as crosslinker after 4 weeks' storage time.

Table 4. Summarized STA data from the cured ϵ CL samples with 5 and 10 mol% DOX/DCL as crosslinker; ΔH_0 represents the melting enthalpy of polycaprolactone according to the literature¹⁷

Crosslinker	Storage	ΔH_0 (J g ⁻¹)	Area (J g ⁻¹)	Melting peak (°C)	Calculated crystallinity (%)
5 mol% DOX	4 weeks	-157	80.2	60	51
10 mol% DOX			28.5	58	18
5 mol% DCL			123.3	66	79
10 mol% DCL			25.8	57	16

more rigid samples are obtained when 5% DCL is used as crosslinker. With proceeding crystallization the strain at break is reduced and the tensile strength increased. The samples with 10 mol% DCL could not be analysed since the material softness made it challenging to remove the fragile samples from the mould.

Shape memory

Specimens with high crystallinity also showed shape memory behaviour upon heating. Similar materials are already known for their shape memory properties.^{8,24,25} For demonstration, a DMTA specimen was prepared, warmed to approximately 70 °C until the material became transparent and flexible and then fixed in a U-shape with a clamp. After cooling, the specimen recrystallized in the new shape (Fig. 10(a)) and remained without any fixation of the material. The sample was then warmed again until it reversed back into the original shape after polymerization (Figs 10(b)–10(d)). This behaviour was observed with 5 mol% DOX as well as 5 mol% DCL. The samples with 10 mol% were too soft and flexible using both crosslinkers.

Hot lithography

Since the light source of the hot lithography printer is a 375 nm laser, adaptations had to be made to make the initiating system compatible with the device. While the selected formulations showed good reactivity using a broadband UV lamp with a light intensity of 67 mW cm⁻², preliminary tests via photorheology with a standard 365 nm light-emitting diode (LED) with an output of 12 mW cm⁻² exhibited only slightly reduced reactivity when a photosensitizer was used. The 365 nm light source was selected due to availability. Literature reports suggested the use of an anthracene-based compound combined with onium salts,²⁶ so 9,10-dibutoxyanthracene was selected since it has better solubility than anthracene and has already been used for hot lithography.^{1,2}

Under these conditions and at 120 °C, the difference between formulations containing 5 and 10 mol% crosslinker in photorheology studies seemed to be negligible (Figs S1, S2 and Table S2). Therefore, both crosslinker ratios were used in initial exposure tests using a Caligma 200 UV hot lithography device from Cubicure, but only with 10 mol% crosslinker was successful curing achieved.

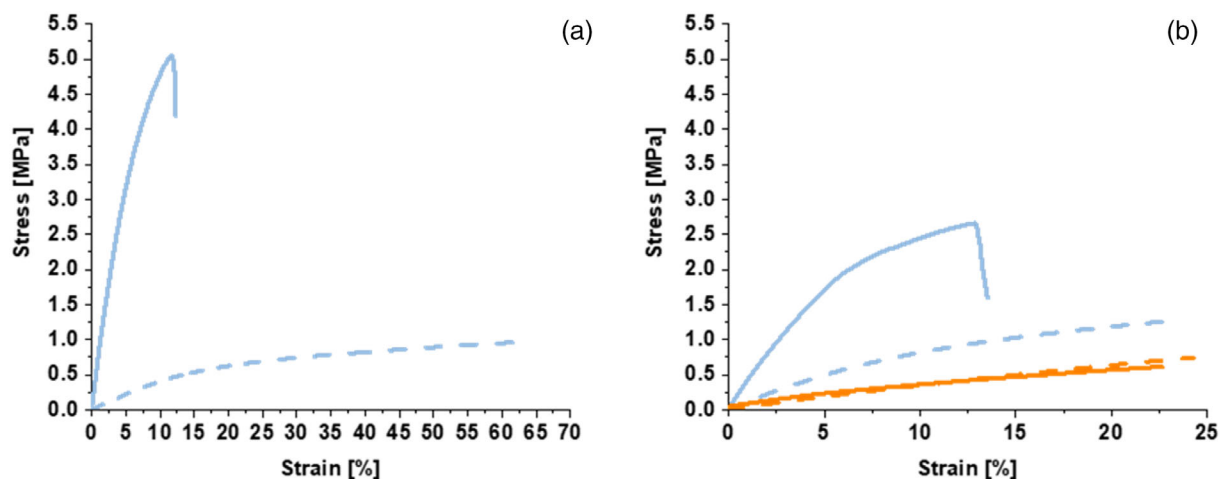


Figure 9. Stress–strain plot for specimens containing (a) ϵ CL and 5% DCL and (b) 5% (light blue) or 10% (orange) DOX after 1 day (broken lines) and 4 weeks (full lines) of storage.

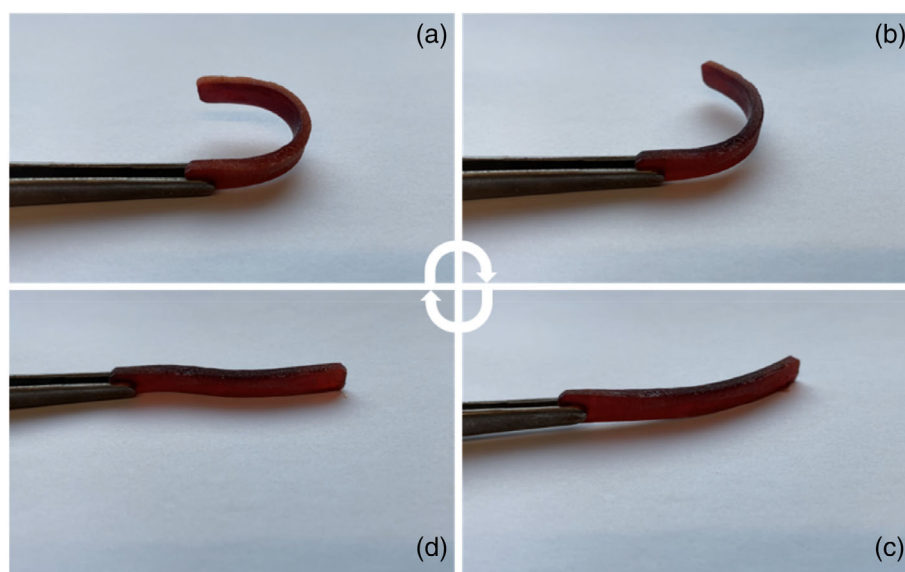


Figure 10. Shape memory properties of a DMTA specimen containing 5 mol% DOX as crosslinker. The polymerized specimen was warmed and fixed in a U-shape to cool down (a). Upon heating (b), (c) it turned back to its original shape (d).

The first exposure tests also revealed that over-polymerization is occurring, which significantly reduces the resolution of the printed parts. To reduce this effect a base was added to inhibit the polymerization that takes place due to the migration of the formed acid outside of the irradiated areas. Based on previous tests ethyl 4-(dimethylamino)benzoate (EDAB) was selected.

After varying the sensitizer and base amount, the first proof of concept could be achieved, where cones consisting of 5–20 layers were printed (Fig. 11). The used formulation contained 90 mol% ϵ CL, 10 mol% DOX, 1 mol% S-B, 0.035 mol% 9,10-dibutoxyanthracene (DBA) and 0.012 mol% EDAB. The mole percent of initiator, base and sensitizer is again relative to the number of combined functional groups from the monomers. One very crucial parameter was the printing temperature. After various tests, the printing was most successful with a vat temperature of 95 °C. In addition, the building platform was first set to 90 °C, but was cooled to 80 °C during printing to improve the attachment of the polymerized samples. While a higher temperature was more beneficial for

the polymerization, it also meant that the printed parts were softer and sometimes detached from the platform during the process. Printing was performed with a speed of 1 m s⁻¹ and each layer was exposed four times with a 375 nm laser.

The cone consisting of 20 layers was also viewed via SEM (Fig. 11). Interestingly, the microscopy does not exhibit any of the 20 layers with a thickness of 50 μ m, but one layer which has the exact thickness of 1 mm. This appearance derives either from post-curing of the printed part where the dark reaction is continued or the self-healing property of the polyester.⁸

CONCLUSION

Polyesters are a highly interesting class of compounds for biomedical applications and hence for 3D printing, since completely individualized parts can be created using stereolithography.

By using cationic ring-opening photopolymerization, we presented a first proof of concept that polyesters can be formed *in*

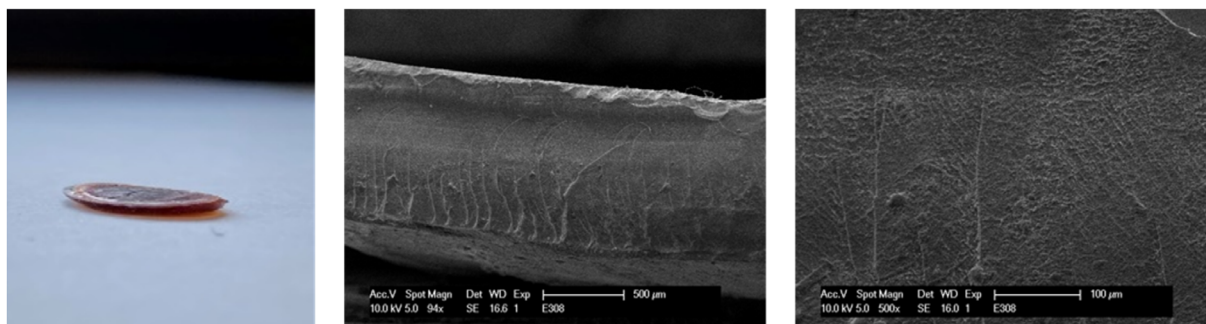


Figure 11. 3D printed cone with 20 layers and a layer thickness of 50 μm , consisting of 90% ϵCL and 10% DOX. The curing was performed using 1% S-B as photoinitiator and 0.035% DBA as photosensitizer.

situ during the 3D printing process, instead of deploying pre-synthesized polyesters. Our photorheology tests showed that ϵCL exhibits good reactivity at high temperature and the introduction of crosslinkers with oxetane (DOX) as well as cyclic ester (DCL) moieties leads to the formation of stable structures and faster gelation. Furthermore, by reducing the amount of crosslinker to 5 mol% we were able to influence the crystallinity of the cured samples and show the shape memory properties of our cross-linked polyester. Tests also showed that post-curing is necessary in order to obtain a stable specimen. We showed that samples with 5 mol% crosslinker develop a high crystallinity, increased T_g and storage modulus as well as tensile strength after a certain storage time, while samples with 10 mol% crosslinker do not exhibit any significant changes. Finally, we were able to print 20 layers using ϵCL with 10 mol% DOX at 120 $^\circ\text{C}$. SEM analysis of the 3D printed part showed that the post-curing process not only increased the conversion but had the positive side effect of creating a smooth transition between the layers.

While the proposition to directly polymerize and print cyclic esters is a very straightforward approach, it also clearly brings various challenges and requires further investigation to be able to compete with the state-of-the-art techniques to print polyesters. The first crucial aspect is the availability of a technique which overcomes the low polymerization rate by performing the printing at temperatures up to 120 $^\circ\text{C}$. At the same time, the initiator stability and monomer volatility need to be considered, which means that not every monomer system will be appropriate. While introducing a crosslinker allows us to decrease the gelation time which is important to obtain a solid and stable structure to which additional layers can be attached, only low amounts of crosslinker lead to polymers with high semicrystallinity. Another characteristic of the cationic photopolymerization—the dark reaction—can lead to issues regarding the resolution of the printed parts. The formation of networks was also seen as a beneficial aspect since it allows the material to degrade but keep its structural integrity during the degradation process. Overall, even though this study forms the basis for the direct printing of polyesters starting from cyclic esters, more investigation is necessary to overcome the problem of over-polymerization and reach even faster polymerization rates with low crosslinker contents.

EXPERIMENTAL/METHODS

Materials and general methods

4,4-Bicyclohexanone (Abcr), 3-chloroperoxybenzoic acid (Sigma Aldrich), 9,10-dibutoxyanthracene (Abcr), bisphenol A diglycidylether (Huntsman) and propiolactone (Abcr) were purchased from

the respective companies and used as received. Caprolactone (TCI) was dried over molecular sieves.

Triarylsulfonium tetrakis(pentafluorophenyl)borate (Irgacure 290) was kindly provided by BASF and used as received. Epoxidized soybean oil was provided by Herwe GmbH and was also used without any additional purification.

NMR analysis was performed with a Bruker Avance at 200 MHz for ^1H NMR and at 50 MHz for ^{13}C NMR. Chemical shifts were referenced to the solvent peak (CDCl_3) in parts per million. The peak multiplicities are described as s (singlet), d (doublet), t (triplet) or m (multiplet).

Synthesis of 5-(7-oxo-4-oxepanyl)-2-oxepanone (DCL)

The synthesis was performed based on literature reports.¹⁶ Bicyclohexanone (6 g, 31 mmol) was dissolved in dichloromethane (80 mL) at room temperatures and 3-chloroperoxybenzoic acid (22.8 g, 93 mmol) was added in several portions while stirring. After stirring overnight, the white precipitate was filtered off and water was added to quench the reaction. The organic phase was extracted with $\text{Na}_2\text{S}_2\text{O}_3$, NaHCO_3 and H_2O and then dried with Na_2SO_4 . The solvent was removed *in vacuo* and the product was obtained as a white solid (80% of theory) after recrystallization in ethyl acetate.

Melting point 175–177 $^\circ\text{C}$. ^1H NMR (200.1 MHz, CDCl_3 , δ): 4.38–4.26, 4.22–4.05 (m, 4H, $-\text{CH}_2-\text{O}-$), 2.8–2.46 (m, 4H, $-\text{CH}_2-\text{C}=\text{O}$), 1.95–1.75 (m, 4H, $-\text{CH}_2-$), 1.7–1.4 (m, 6H, $-\text{CH}_2-$). ^{13}C NMR (50.3 MHz, CDCl_3 , δ): 175.4 (C4), 68.0 (C2), 45.9 (C1), 33.3 (C2), 32.1 (C2), 25.8 (C2).

Preparation of resin formulations

The formulations for the photorheology analysis were prepared by mixing 5 or 10 mol% of crosslinker with 95%/90% of ϵCL . Then 1 mol% of photoinitiator (S-B) relative to the number of functional groups was added and dissolved. In the case of DCL, the formulation was heated to 70 $^\circ\text{C}$ to improve the dissolution. Formulations for the preparation of specimens for mechanical testing were prepared similarly.

Photorheology

Photorheology studies were performed with an Anton Paar MCR 302 WESP device, equipped with a P-PTD 200/GL Peltier glass plate and a PP25 measuring system. As light source an Exfo Omni-Cure TM 2000 device (320–500 nm) with an output of 80 mW cm^{-2} on the sample surface was used. For each measurement, a polyethylene tape was placed on the glass plate and the surface was heated to the selected temperature. Using a tape was necessary since removing the polymerized sample proved

to be difficult for epoxy monomers. To have comparable conditions, the tape was used for all monomers. Then 120 μL of monomer mixture was placed on the plate and sheared with a strain of 1% and a frequency of 1 Hz. Every formulation was measured three times for each temperature. Additional runs were made in case the measurements showed low reproducibility.

The values for t_{gel} were determined by the intersection of the storage (G') and loss (G'') moduli curves. The results for G'_{final} were obtained by using the average of the last 10 points from the measurement. Conversion analysis via near IR was not performed since no clear changes in absorption could be observed.

Specimen preparation

Specimens for the mechanical tests were prepared by placing the formulation into silicon moulds ($5 \times 2 \times 40 \text{ mm}^3$) which were coated with a Teflon spray. The curing was performed in a Uvitron UV 1080 Flood Curing Oven equipped with Uvitron Intelliray 600 halide lamps at 50% intensity (which corresponds to approximately 60 mW cm^{-2} on the surface of the sample) with a spectral range from 320 to 580 nm for 20 min. Then the specimens were post-cured in an oven at 110 $^{\circ}\text{C}$ for 2 h. Before cooling to room temperature, the specimens were first placed in an oven with a temperature of 50 $^{\circ}\text{C}$ for an additional 30 min in order to prolong the cooling time.

Dynamic mechanical thermal analysis (DMTA)

DMTA was performed using an Anton Paar MCR 301 device with a CTC 450 oven. The specimens were measured in torsion mode with a frequency of 1 Hz and a strain of 0.1%. The temperature was increased from -100 to $200 \text{ }^{\circ}\text{C}$ with a heating rate of $2 \text{ }^{\circ}\text{C min}^{-1}$. The glass transition temperature was defined as the temperature at the maximum loss factor ($\tan \delta$).

Tensile tests

The samples for the tensile tests were prepared analogously to the DMTA specimens according to the requirements for ISO 527 test specimen 5b (a $2 \times 2 \times 12 \text{ mm}^3$ parallel region, a total length of 35 mm). The study was performed on a Zwick Z050 with a maximum test force of 100 N. The specimens were fixed by using two clamps and strain was applied with a speed of 5 mm min^{-1} . Simultaneously, a strain–stress curve was recorded for analysis.

Conversion analysis

Three samples (ca 20–25 mg) of each cured DMTA specimen were put into different vials with 1 mL of MEK. After 24 h the sample was removed, washed with fresh MEK and dried for 24 h. The MEK solutions were combined and the solvent was evaporated. The residue was then dissolved in CDCl_3 and NMR analysis was conducted. Subsequently, the CDCl_3 was evaporated and the residue was again dissolved in tetrahydrofuran. The solution was transferred to a vial via a syringe filter and GPC analysis was performed to determine the molecular weight.

Gel permeation chromatography (GPC)

For GPC analysis the cured samples were dissolved in tetrahydrofuran (yielding concentrations of about 5 mg mL^{-1}) containing 0.5 mg mL^{-1} butylated hydroxytoluene as a flow marker and transferred into GPC vials via syringe filters. The measurements were conducted with a Malvern VISCOTEK TDA device equipped with three columns which were connected in series, a UV Detector Module 2550 for TDA 305 and a VISCOTEK SEC-MALS 9 light

scattering detector. The molecular weight was evaluated using conventional calibration with polystyrene standards (375–177 000 Da).

Simultaneous thermal analysis (STA)

The analysis was performed with an STA 449 F1 Jupiter device from Netzsch. Small samples of approximately 15–20 mg were cut off the DMTA specimens, weighed in aluminium crucibles and closed with pierced aluminium lids. The polymer samples were heated at a rate of 10 K min^{-1} from 25 to $200 \text{ }^{\circ}\text{C}$ under an N_2 atmosphere (flow rate 40 mL min^{-1}). During the heating, the calorimetric information as well as gravimetric changes were recorded and subsequently analysed with the Netzsch Proteus thermal analysis software. To calculate the crystallinity the melting enthalpy was compared to literature values for 100% crystalline polymers.¹⁷

Hot lithography

The 3D printing was performed on the hot lithography device Caligma UV from the company Cubicure GmbH. The $90 \text{ }^{\circ}\text{C}$ pre-heated monomer was heated to $95 \text{ }^{\circ}\text{C}$ in the vat and the building platform was first set to $90 \text{ }^{\circ}\text{C}$ and subsequently cooled to $80 \text{ }^{\circ}\text{C}$ during the printing process, to improve the attachment of the cured polymer to the platform. The formulation consisted of 90% ϵCL and 10% difunctional oxetane (DOX). The initiator S-B (1 mol%), photosensitizer DBA (0.035 mol%) and base EDAB (0.012 mol%) were all added relative to the number of functional groups. The cones were printed using a 375 nm laser with an energy density of 2320 mJ cm^{-2} and a layer thickness of $50 \mu\text{m}$. Different cones with layer numbers from 5 to 20 could be successfully printed.

ACKNOWLEDGEMENTS

The authors would like to thank BASF for the supply of Irgacure 290 and Herwe GmbH for providing epoxidized soybean oil.

CONFLICT OF INTEREST

The authors declare no competing financial interest.

SUPPORTING INFORMATION

Supporting information may be found in the online version of this article.

REFERENCES

- Dall'Argine C, Hochwallner A, Klikovits N, Liska R, Stampf J and Sangermano M, *Macromol Mater Eng* **305**:2000325 (2020).
- Klikovits N, Sinaweil L, Knaack P, Koch T, Stampf J, Gorsche C *et al.*, *ACS Macro Lett* **9**:546–551 (2020).
- Wolff R, Ehrmann K, Knaack P, Seidler K, Gorsche C, Koch T *et al.*, *Polym Chem* **13**:768–777 (2022).
- Sangermano M, Tonin M and Yagci Y, *Eur Polym J* **46**:254–259 (2010).
- Barker IA and Dove AP, *Chem Commun* **49**:1205–1207 (2013).
- Fu C, Xu J and Boyer C, *Chem Commun* **52**:7126–7129 (2016).
- Zayas MS, Dolinski ND, Self JL, Abdilla A, Hawker CJ, Bates CM *et al.*, *ChemPhotoChem* **3**:467–472 (2019).
- Bener S, Yilmaz G and Yagci Y, *ChemPhotoChem* **5**:1089–1093 (2021).
- Mete Y, Knaack P and Liska R, *Polym Int* **71**:797–803.
- Mondschein RJ, Kanitkar A, Williams CB, Verbridge SS and Long TE, *Biomaterials* **140**:170–188 (2017).
- Invernizzi M, Turri S, Levi M and Suriano R, *Eur Polym J* **101**:169–176 (2018).

- 12 Elomaa L, Kokkari A, Närhi T and Seppälä JV, *Compos Sci Technol* **74**:99–106 (2013).
- 13 Seppälä J, Korhonen H, Hakala R and Malin M, *Macromol Biosci* **11**: 1647–1652 (2011).
- 14 Thompson JR, Worthington KS, Green BJ, Mullin NK, Jiao C, Kaalberg EE *et al.*, *Acta Biomater* **94**:204–218 (2019).
- 15 Lammel-Lindemann J, Dourado IA, Shanklin J, Rodriguez CA, Catalani LH and Dean D, *Bioprinting* **18**:e00062 (2020).
- 16 Matsuda T and Mizutani M, *J Biomed Mater Res* **62**:395–403 (2002).
- 17 Michlovská L, Vojtová L, Mravcová L, Hermanová S, Kučerík J and Jančář J, *Macromol Symp* **295**:119–124 (2010).
- 18 Jansen J, Boerakker MJ, Heuts J, Feijen J and Grijpma DW, *J Controlled Release* **147**:54–61 (2010).
- 19 Palmgren R, Karlsson S and Albertsson A-C, *J Polym Sci Part A Polym Chem* **35**:1635–1649 (1997).
- 20 Gorsche C, Harikrishna R, Baudis S, Knaack P, Husar B, Laeuger J *et al.*, *Anal Chem* **89**:4958–4968 (2017).
- 21 Khan SA, Plitz IM and Frantz RA, *Rheol Acta* **31**:151–160 (1992).
- 22 Peer G, Dorfinger P, Koch T, Stampfl J, Gorsche C and Liska R, *Macromolecules* **51**:9344–9353 (2018).
- 23 Wunderlich B, *Pure Appl Chem* **67**:1019–1026 (1995).
- 24 Lowe JR, Tolman WB and Hillmyer MA, *Biomacromolecules* **10**:2003–2008 (2009).
- 25 Utroša P, Onder OC, Žagar E, Kovačič S and Pahovnik D, *Macromolecules* **52**:9291–9298 (2019).
- 26 Crivello J and Jang M, *J Photochem Photobiol, A* **159**:173–188 (2003).